Ultra-relativistic Electrons in the Van Allen Radiation Belts

Yuri Shprits[1,2]

Graduate students and postdoctoral scholars: Dmitri Subbotin[1], Marianne Daae[1], Ksenia Orlova[1], Kyung-Chan Kim[1], Binbin Ni[1], Xudong Gu[1], Alexander Drozdov[1]

Collaborators: Adam Kellerman[1], Maria Spasojevic[3], Dmitri Kondrashov[1] , Drew Terner[1]

[1] Department of Earth and Space Sciences, UCLA

[2]Skolkovo Institute of Sciene and Technology, Russia and Department of Earth Atmospheric and Planetary Sciences, MIT

[3]Stanford University

10/2/2014

Inner Magnetosphere Coupling III (IMC-III) Workshop

23 – 27 March 2015
UCLA

Abstracts due: 20 Dec 2014
Registration: 20 Dec 2014
Early Bird: 23 Oct 2014

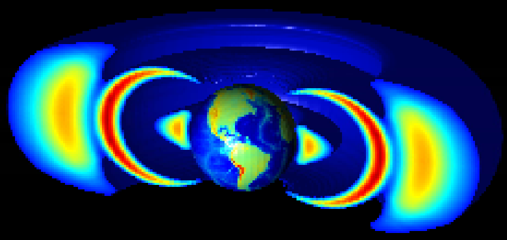

The Inner Magnetosphere Coupling III (IMC-III) workshop will bring together researchers to examine and discuss the strongly coupled inner magnetospheric system and how disturbances from the Sun can propagate to the inner magnetosphere, radically altering the plasma and wave distributions, and ultimately influence the ionosphere and upper atmosphere.

Discussion Topics	Discussion Leaders
Solar wind and magnetosphere	*D. Baker, T. Pulkkinen*
Plasmasphere, ring current, and radiation belts	*M. Chen, M. Liemohn*
Plasma and magnetic field	*C. Lemon, V. Jordanova*
Waves in plasma	*N. Meredith, W. Li*
Plasma sheet injections	*N. Ganushkina, M. Gkioulidou*
Combining models and observations	*M. Hudson, S. Elkington*
Innovative methods for data analysis	*D. Turner, S. Claudepierre*
Mission Synergy	*Y. Miyoshi, A. Runov, H. Spence*
Ionosphere-Thermosphere-Magnetosphere	*M. Moldwin, D. Welling*
Space Weather and Applications	*J. Green, M. Wiltberger*

Theoretical Flux Profiles at Fixed Energy

Two-Zone Structure

Underestimated the Inner Zone Fluxes

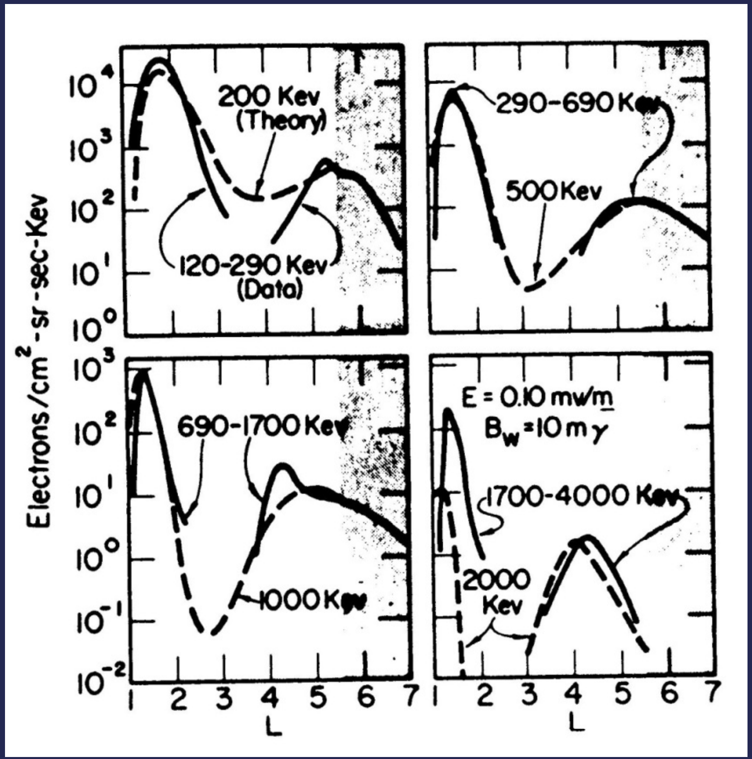

Realistic amplitudes in the outer zone
Successfully reproduced the slot region

$$\frac{\partial f}{\partial t} = L^2 \frac{\partial}{\partial L}\left[D_{LL} L^{-2} \frac{\partial f}{\partial L} \right] - \frac{f}{\tau_{effective}}$$

$$J(E,\alpha) = f(\mu, J, L^*) p^2$$

Electron profiles obtained from the modeling of the quiet time inward radial diffusion and loss.

Theoretical profiles of fluxes agree with observations.

Lyons and Thorne, 1973

Lyons, Thorne, and Kennel, 1972

Competition Between Acceleration and Loss

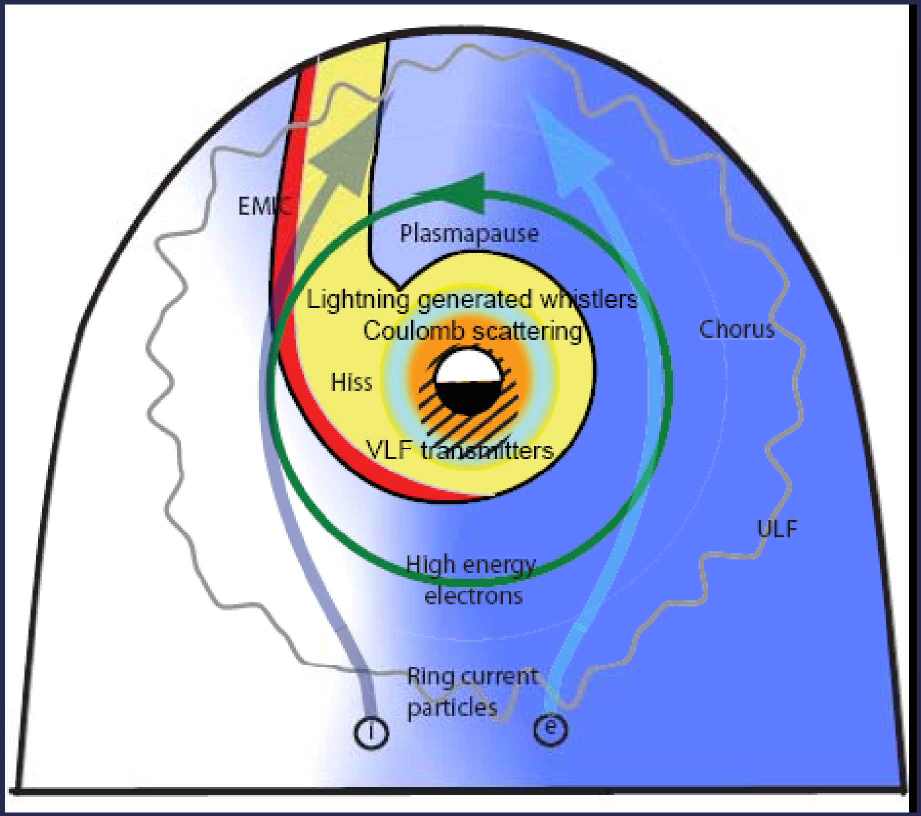

Inward radial diffusion driven by the ULF magnetic fluctuations.

Energy and pitch angle scattering due to resonance interactions with different waves.

Combined effect of losses to magnetopause and outward radial diffusion.

[Shprits et al., 2008; Review JASTP]

3D Fokker Planck Equation including the Mixed Diffusion Terms.

$$
\begin{aligned}
\frac{\partial f}{\partial t} = \quad & L^{*2} \left.\frac{\partial}{\partial L^*}\right|_{J_1,J_2} \frac{1}{L^{*2}} D_{L^*L^*} \left.\frac{\partial f}{\partial L^*}\right|_{J_1,J_2} + \\
& + \frac{1}{p^2} \left.\frac{\partial}{\partial p}\right|_{L,\alpha_0} p^2 \left(D_{pp} \left.\frac{\partial f}{\partial p}\right|_{L,\alpha_0} + D_{p\alpha_0} \left.\frac{\partial f}{\partial \alpha_0}\right|_{L,p} \right) + \\
& + \frac{1}{T(\alpha_0)\sin(2\alpha_0)} \left.\frac{\partial}{\partial \alpha_0}\right|_{L,p} T(\alpha_0)\sin(2\alpha_0) \left(D_{\alpha_0 p} \left.\frac{\partial f}{\partial p}\right|_{L,\alpha_0} + D_{\alpha_0\alpha_0} \left.\frac{\partial f}{\partial \alpha_0}\right|_{L,p} \right) + \\
& + Sources - Losses
\end{aligned}
$$

Pitch-angle and energy diffusion coefficients due to resonant wave-particle interactions

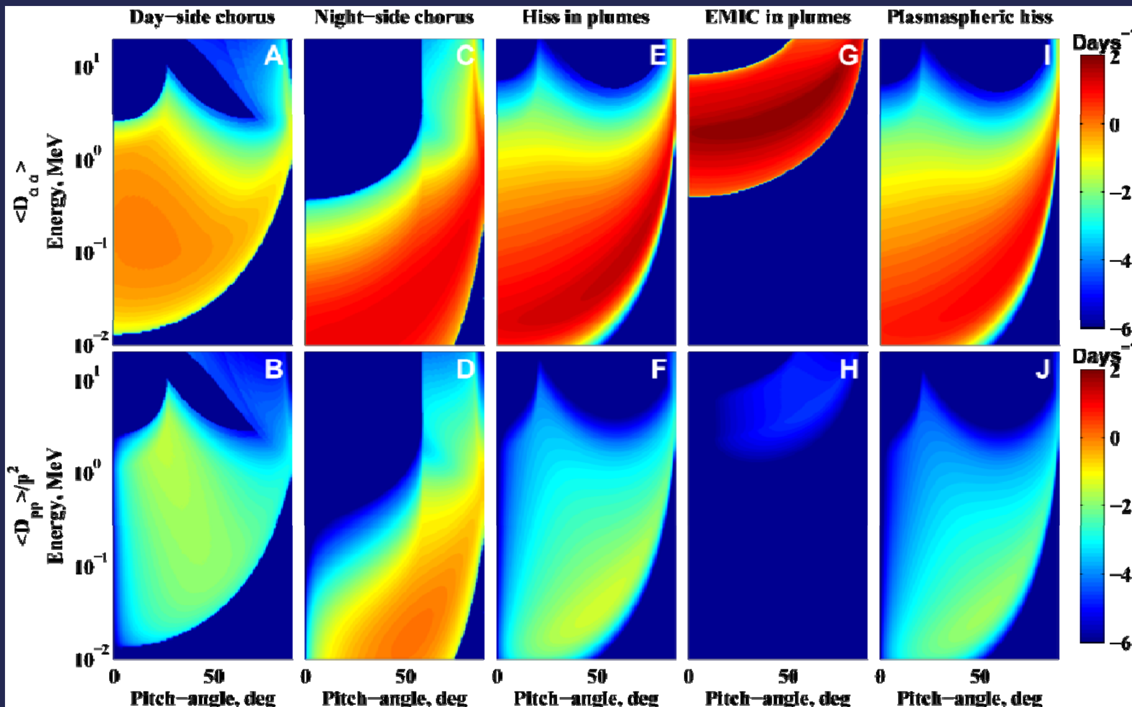

Pitch-angle diffusion results in a loss to the atmosphere

Energy diffusion can locally
accelerate electrons

4D Matrix: geomagnetic activity, radial distance, pitch angle, energy

Diffusion rates due to resonant wave particle interactions with various plasma waves using the FDC code [Shprits and Ni, 2009]. We set up latitudinal distribution of power, wave-normal angle, density. MLT dependent frequency spectrum, wave power as function activity, radial distance, and latitude. Use realistic 3D magnetic field lines.

Validation of the Versatile Electron Radiation Belt (VERB) Code for Over 100 Days in 1990

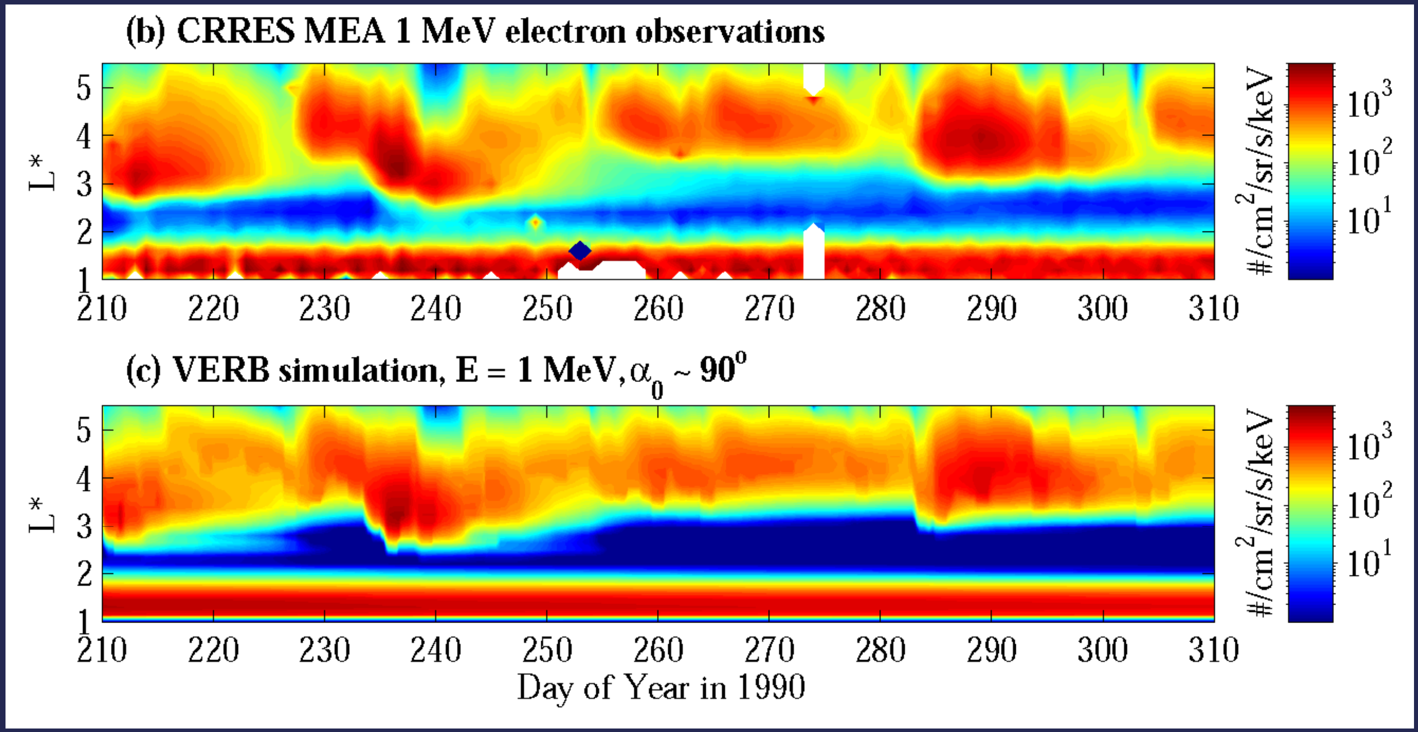

[Kim et al., 2010]

- VERB predicts the instantaneous location of the upper boundary of the slot region, the empty slot region, the stable inner belt, the location of the peak of fluxes and the amplitude of fluxes.

Observations (a) and Modeling (b) of the 2003 Halloween Storms

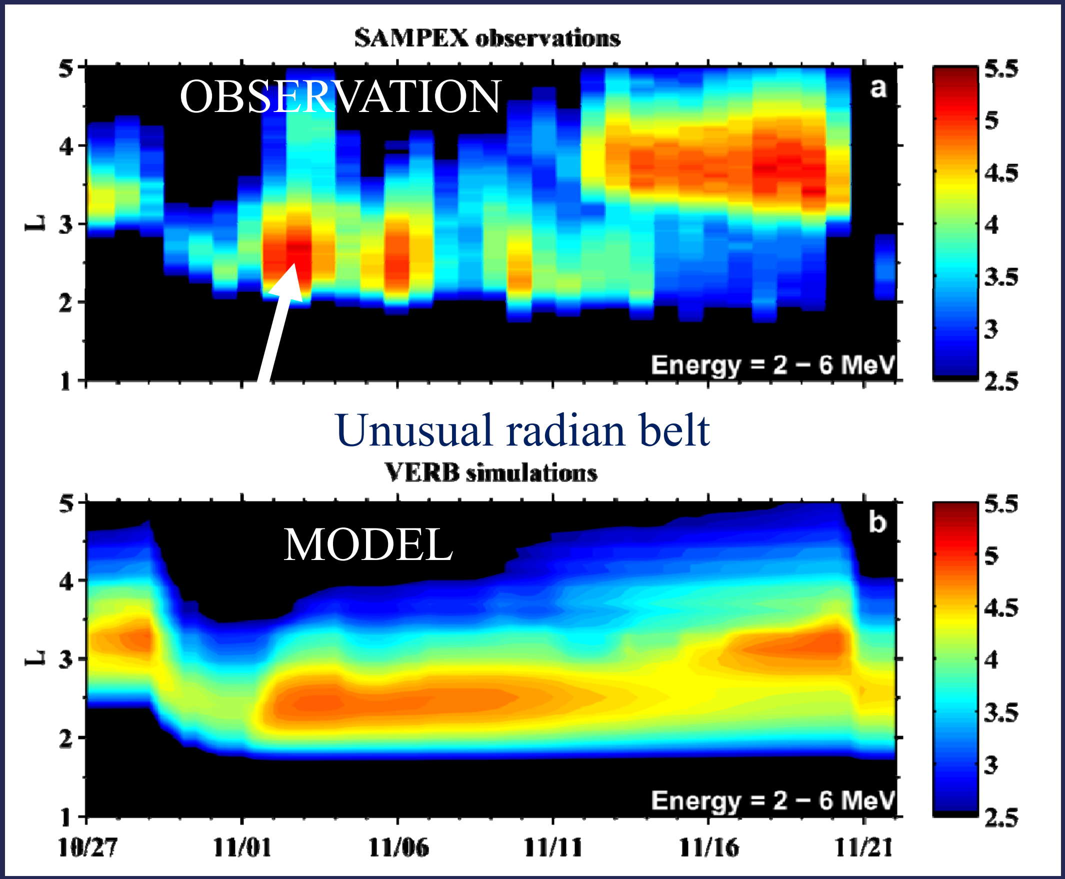

VERB code which now includes radial transport, pitch-angle scattering, and mixed diffusion scattering can reproduce the formation of the unusual radiation belt. The new belt is formed in the slot region which is usually devoid of killer electrons.

[Shprits et al., 2011]

Acceleration of electrons to relativistic energies

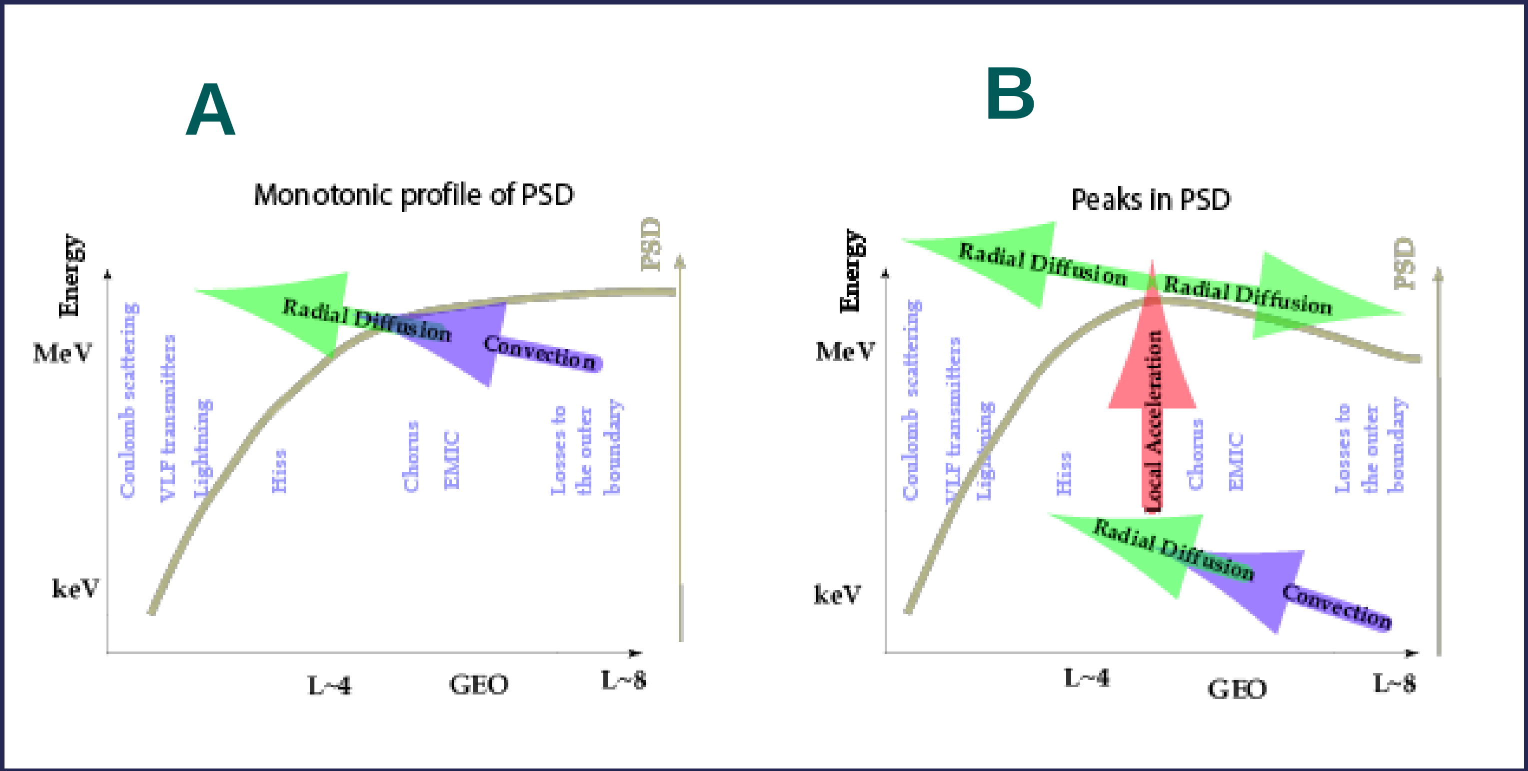

[Shprits et al., 2009]

Observations of the Unusual Storage Ring

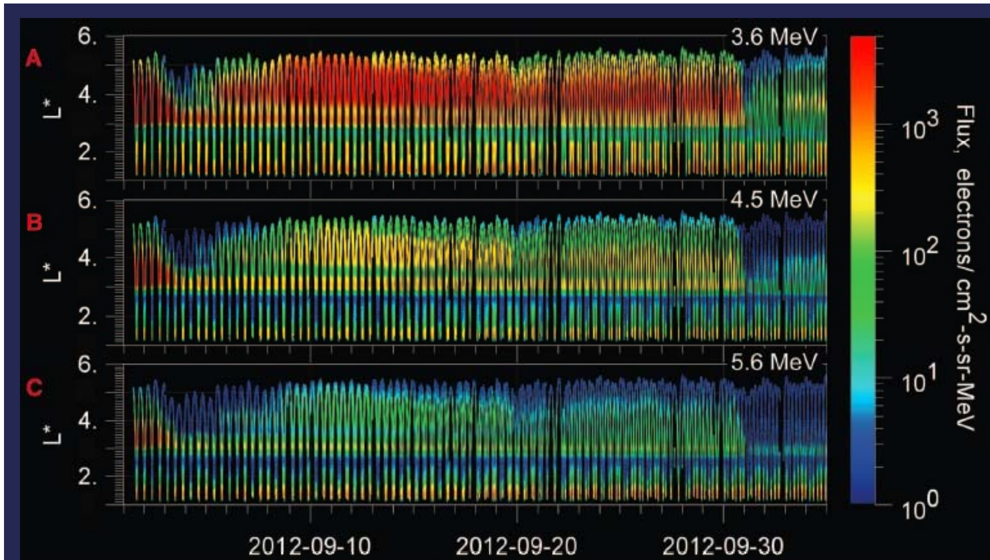

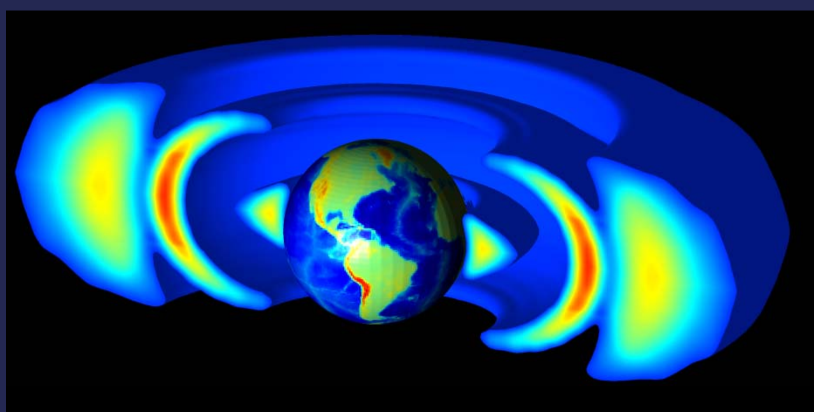

- Third narrow ring was formed on Sept 1st-3rd.
- The structure was very narrow (fraction of Earth radii)
- The ring lived for approximately 1 month until the arrival of the next CME.

Baker et al., 2013 , *Science*

Simulations of loss to MP and 3 diffusive processes

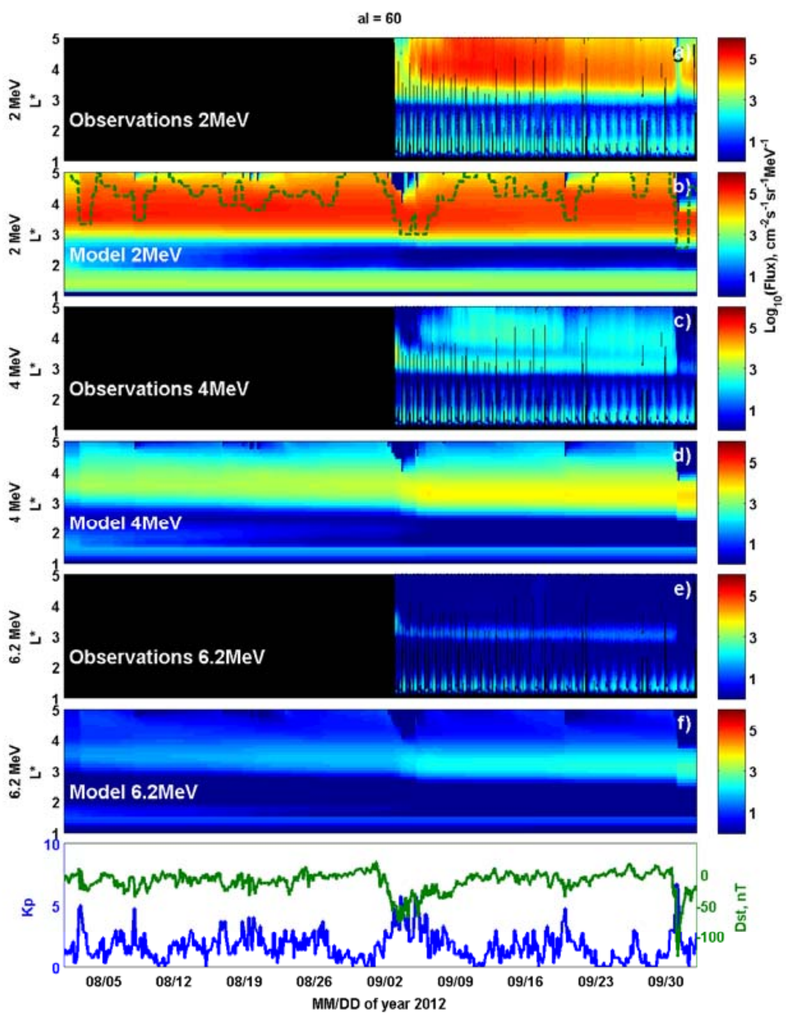

- •Magnetopause loss that can explain for the loss of particles at relativistic energies can not explain losses at ultra-relativistic energies.
- •Additional loss process is required to produce a narrow ring of radiation.

Shprits et al., 2013 *Nature Physics*

EMIC wave observationds

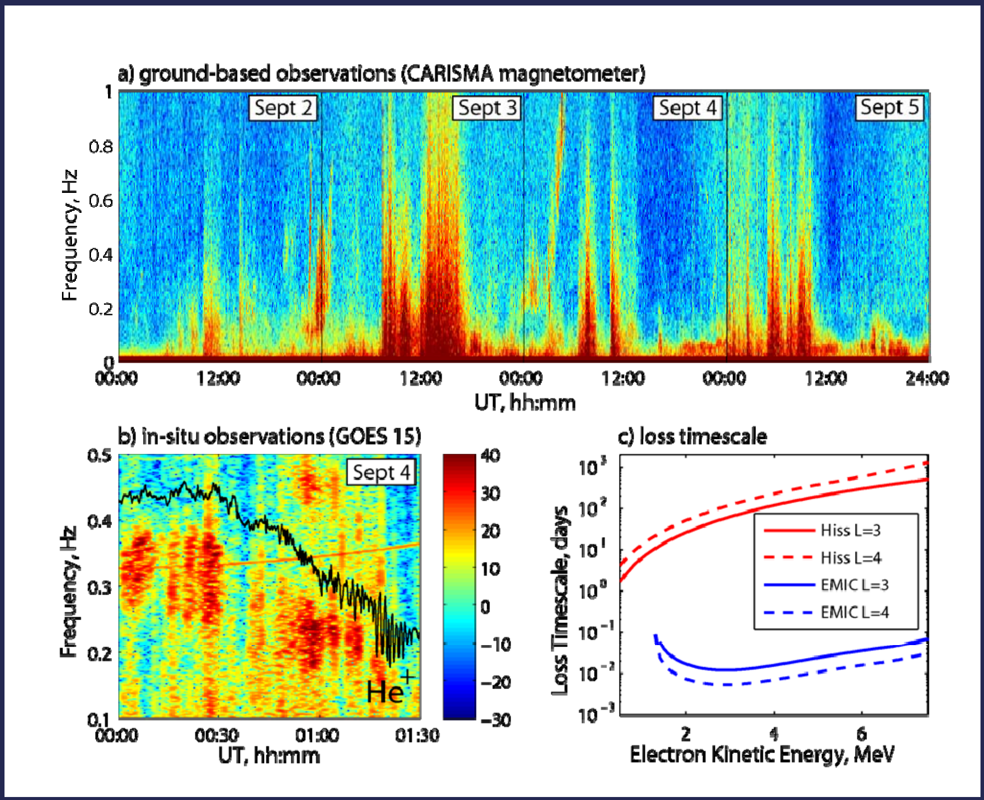

EMIC waves are observed on the ground during the main phase of the storms.

In situ observations of waves

Shprits et al., 2013 *Nature Physics*

Data provided by M Usanova, U of A

Chorus, hiss, EMIC, radial diffusion

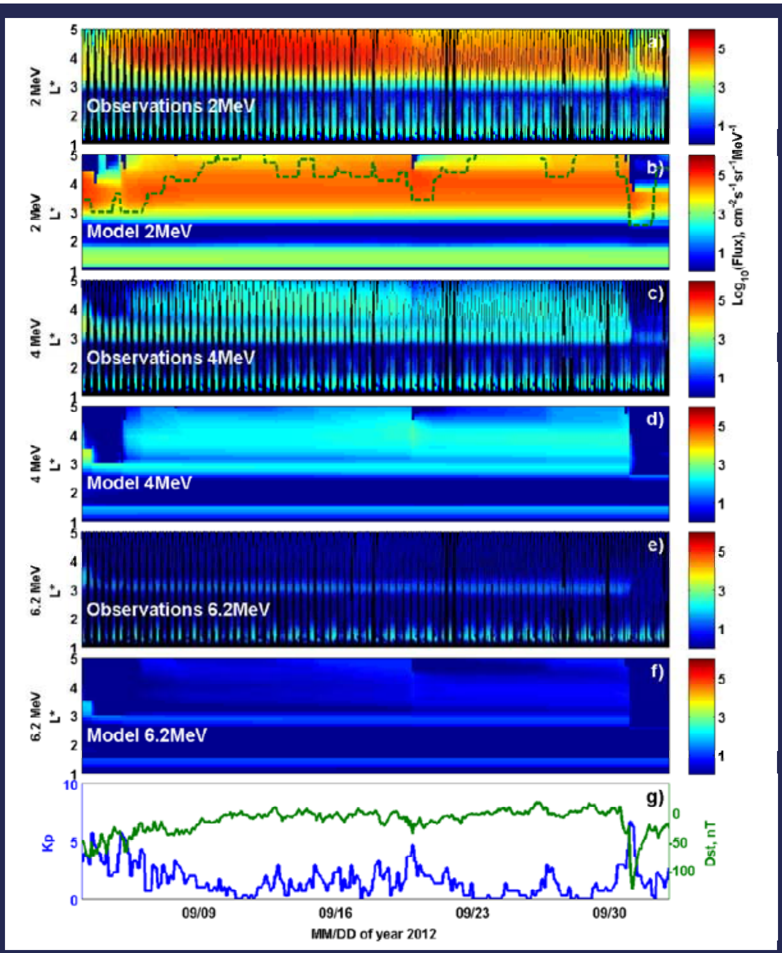

Depletion occurs down to the outer boundary of the plasmapause.

Narrow ring persists until the arrival of the next CME.

Shprits et al., 2013 *Nature Physics*

Physical Explanation of why Hiss Scattering is Inefficient at These Energies

$\omega - k_{||} v_{||} = n\Omega_{gyro}/\gamma.$

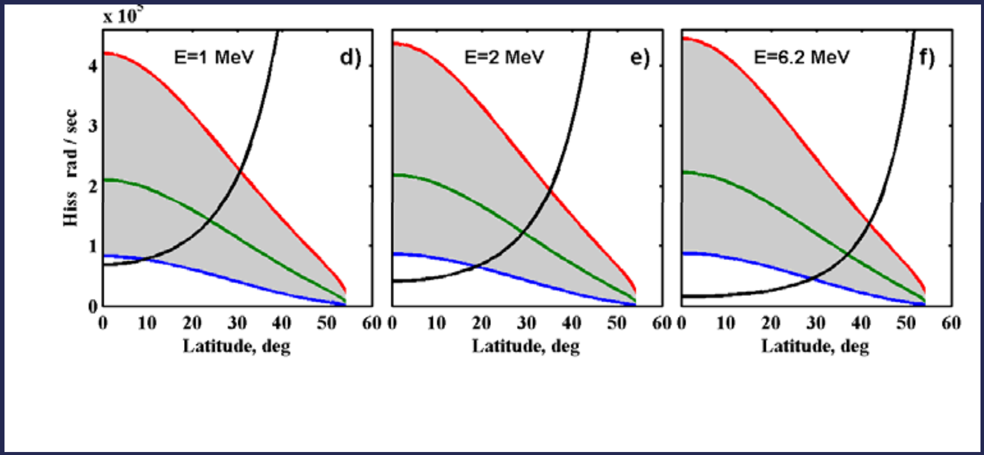

Electrons having energy above 2MeV are out of the resonance with chorus waves at the equator, and cannot be effectively accelerated by chorus waves.

[Shprits et al., 2013, *Nature Physics*]

Computed Electron Pitch-Angle Diffusion

Parameters for the electron pitch-angle diffusion estimate:
$B = 330\ nT$; $n_e = 150\ cm^{-3}$;
$B_{EMIC} = 2\ nT$; $f_{EMIC} = 0.7\text{-}1.1\ Hz$ - *RBSP*

MLT extent: 80% of drift orbit

Ion composition:
70% H^+; *20%* He^+; *10%* O^+ } *assumption*

Computed pitch-angle diffusion coefficients (a-c) and observed normalized electron flux as a function of pitch-angle (d-f) in the 2.3, 4.5, and 7.15 MeV for October 9-13, 2012.

[Usanova, M.E., A. Drozdov, K. Orlova, I. R. et al., 2014]

Long Term Simulations at Relativistic Energies

Modeling can reproduce the general dynamics of the radiation belts at Relativistic Energies

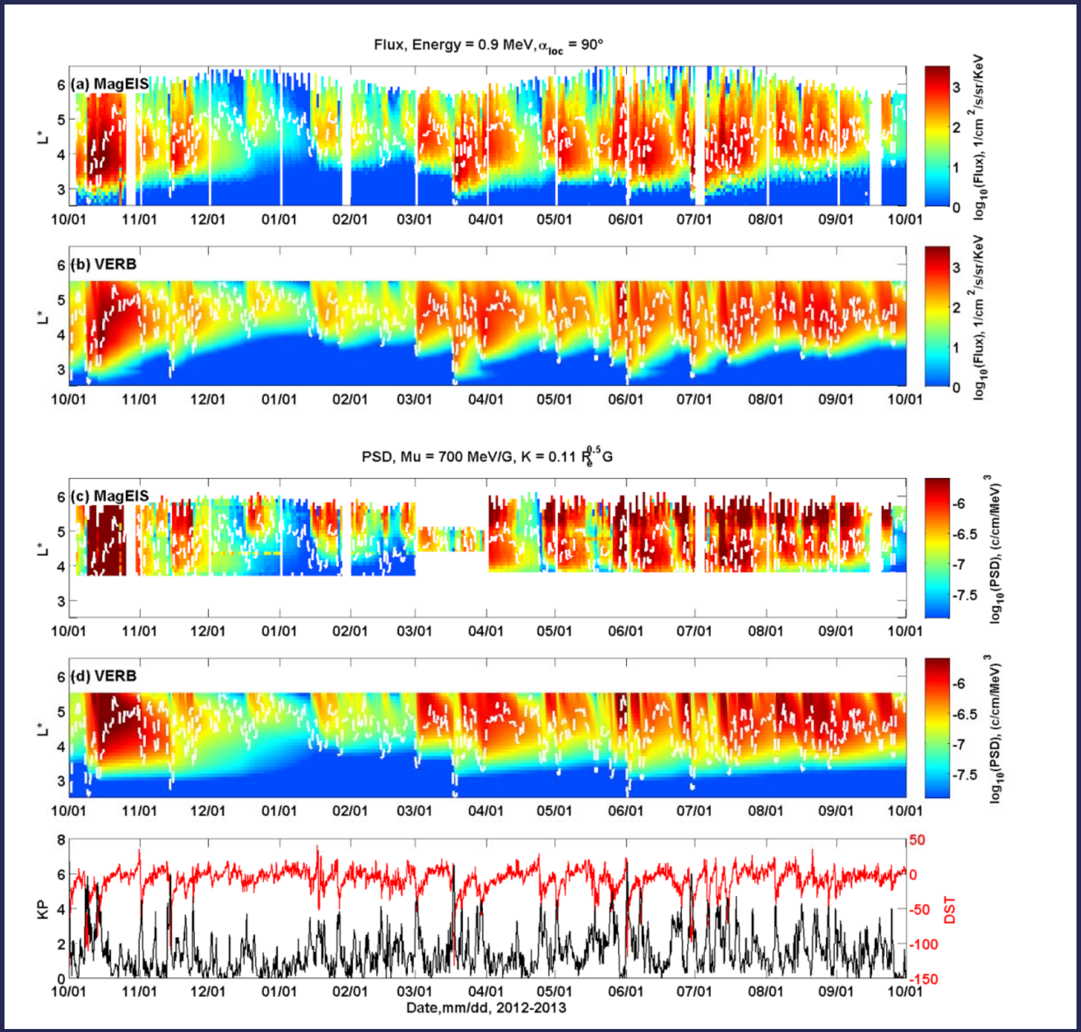

Long Term Simulations of the Ultra-Relativistic Electrons

Modeling cannot reproduce the general dynamics of the radiation belts at Ultra-Relativistic Energies. Additional loss mechanisms are required

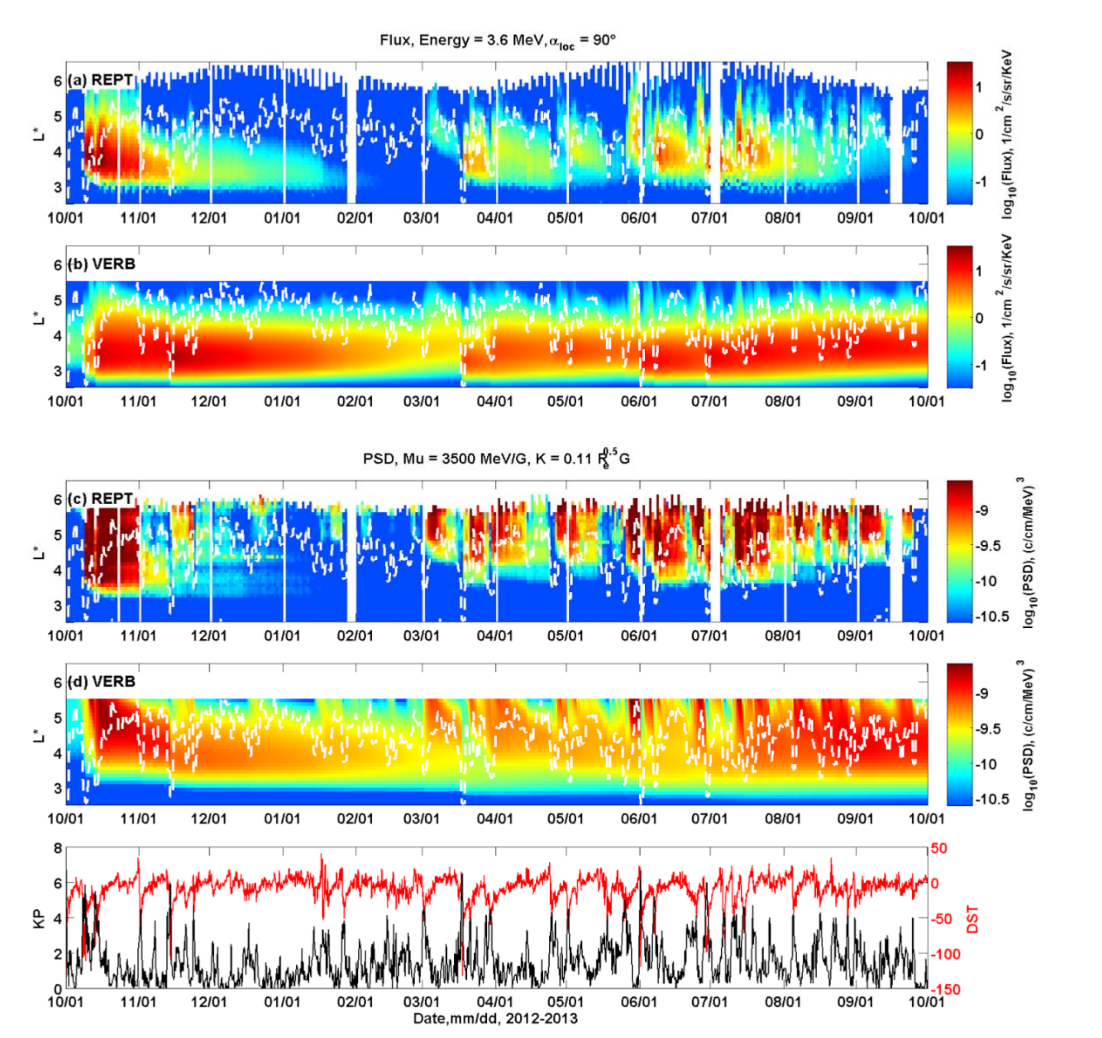

Decay Rates at 100keV and 300keV

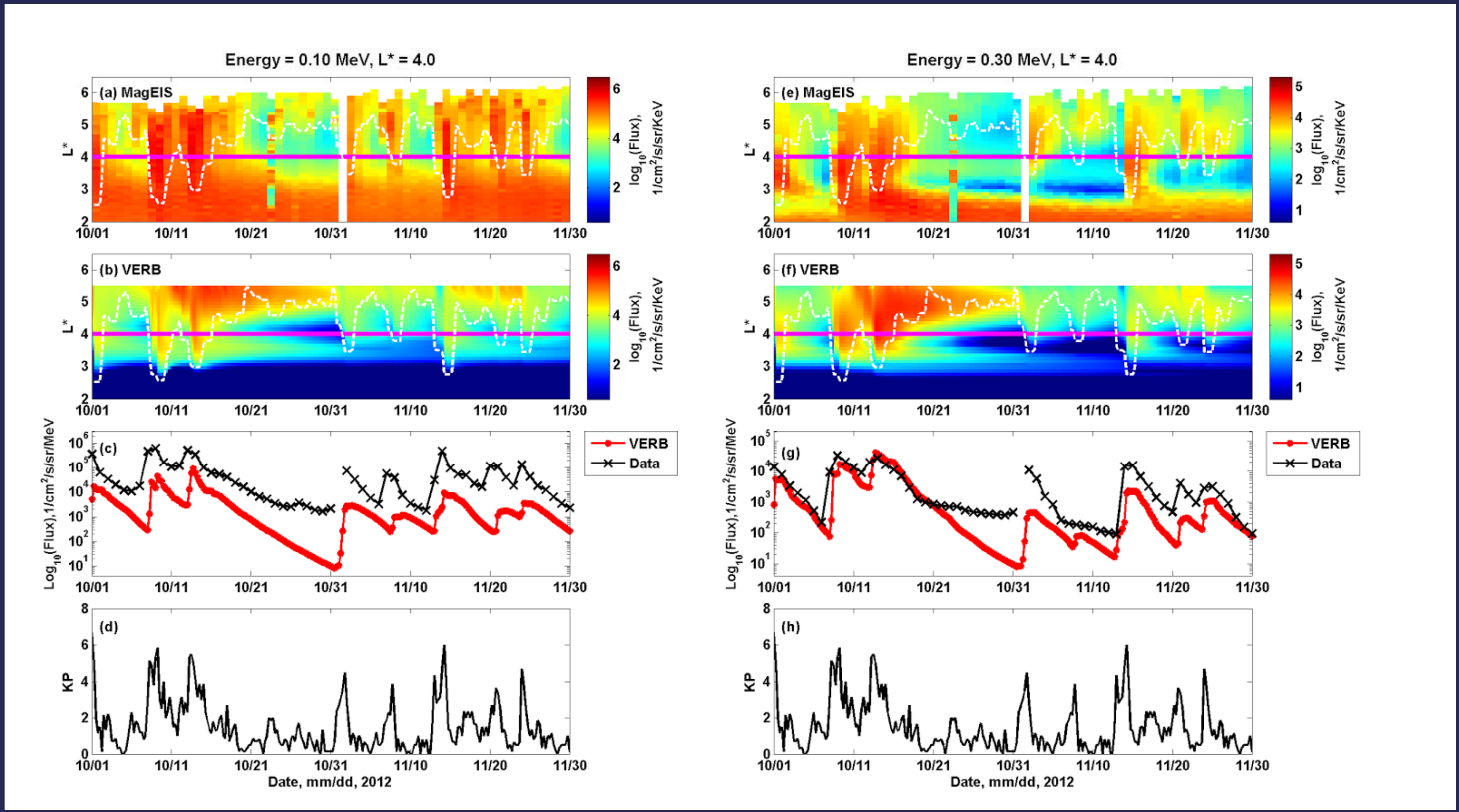

Decay Rates at

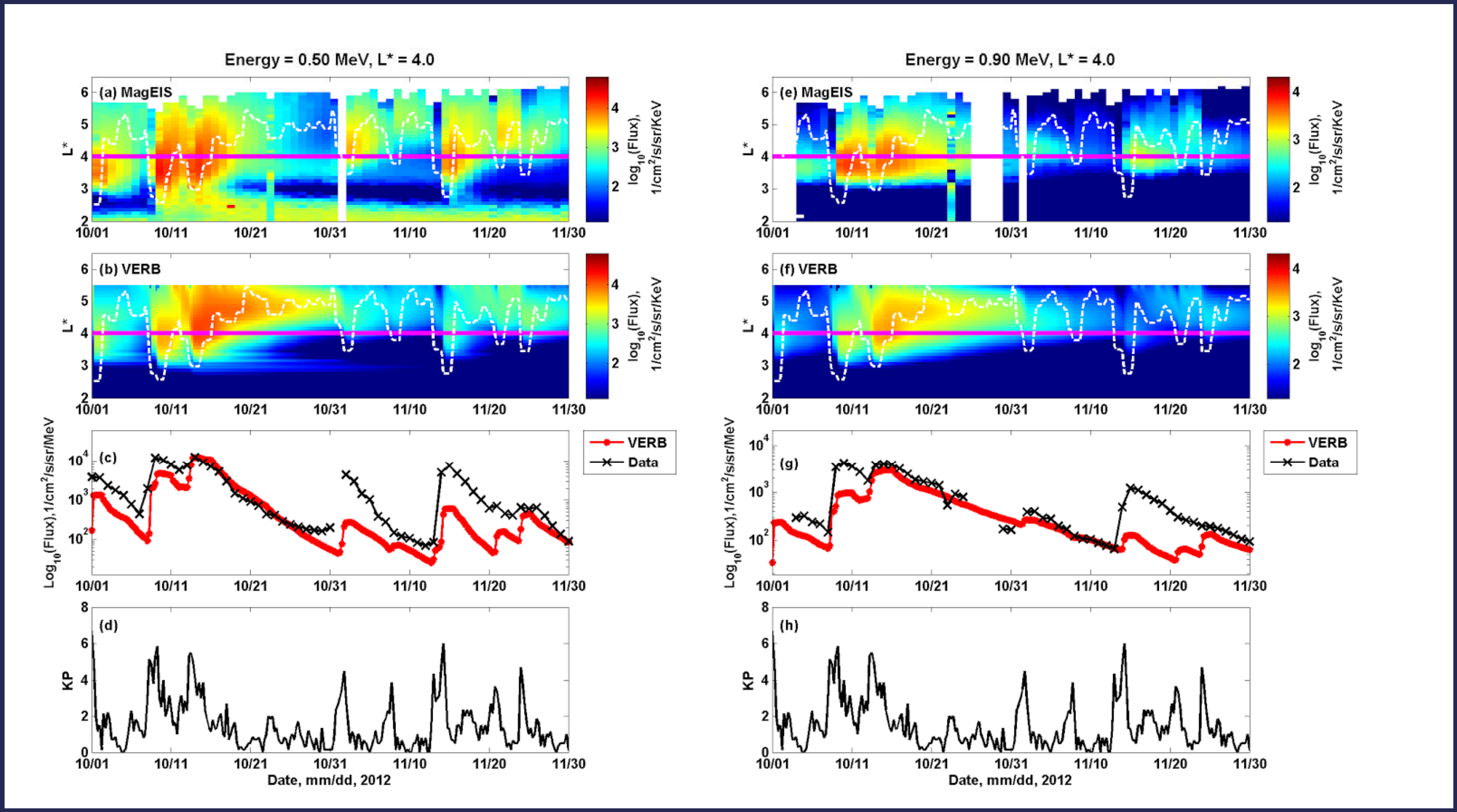

Decay Rates at 2 MeV and 3.6 MeV

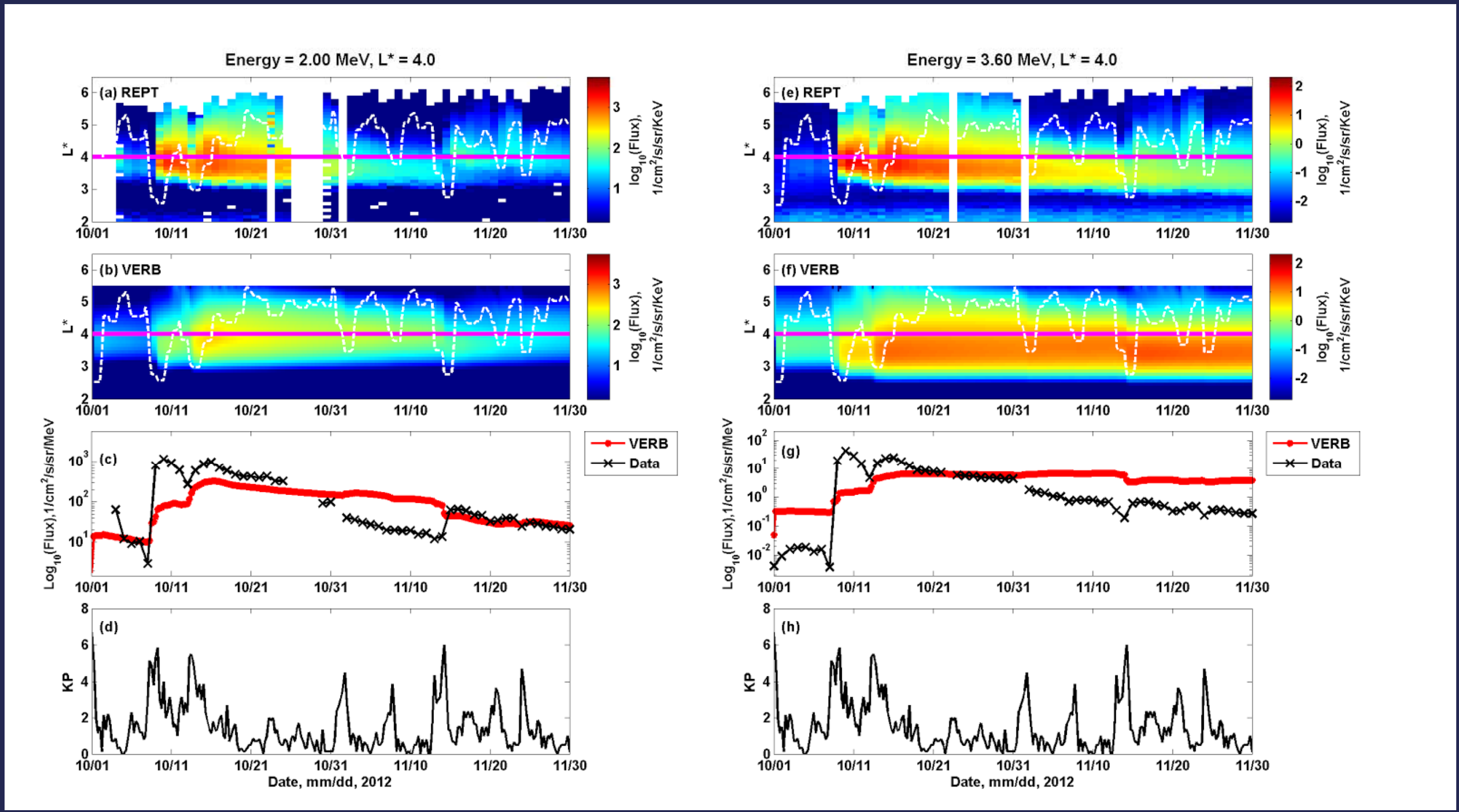

Conditions for Efficient Acceleration of Ultra-Relativistic Electrons in the Outer Radiation Belt, October 8-9, 2012

•A prolonged period of enhanced convection, which injects plasma sheet electrons into the inner magnetosphere leading to an enhanced source population of 30-100 keV electrons, lower total plasma density, and the excitation of intense whistler mode chorus in the low density region outside the plasmasphere.

Evidence for peaks in PSD,
Reeves et al., Science 2013

October 8-9, 2012

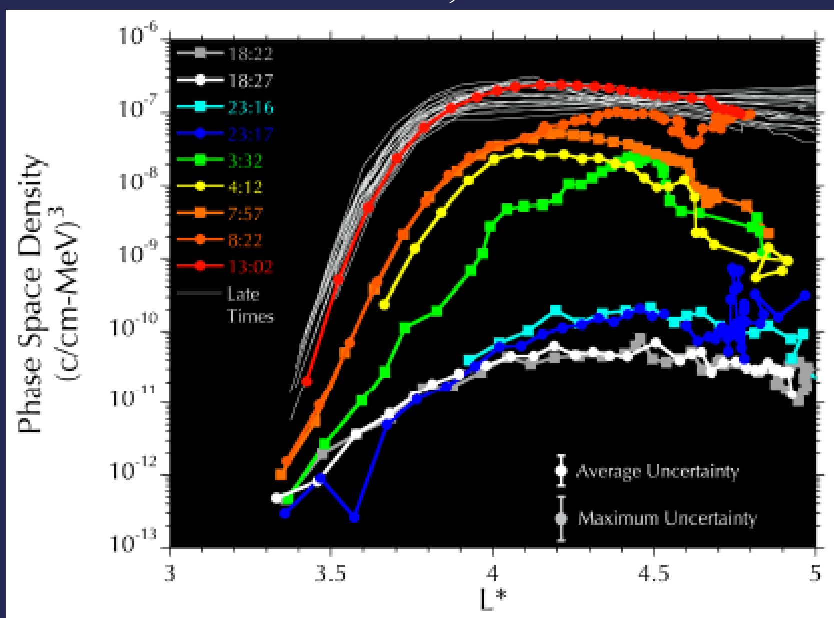

Simulation of electron acceleration
Thorne et al., Nature 2013

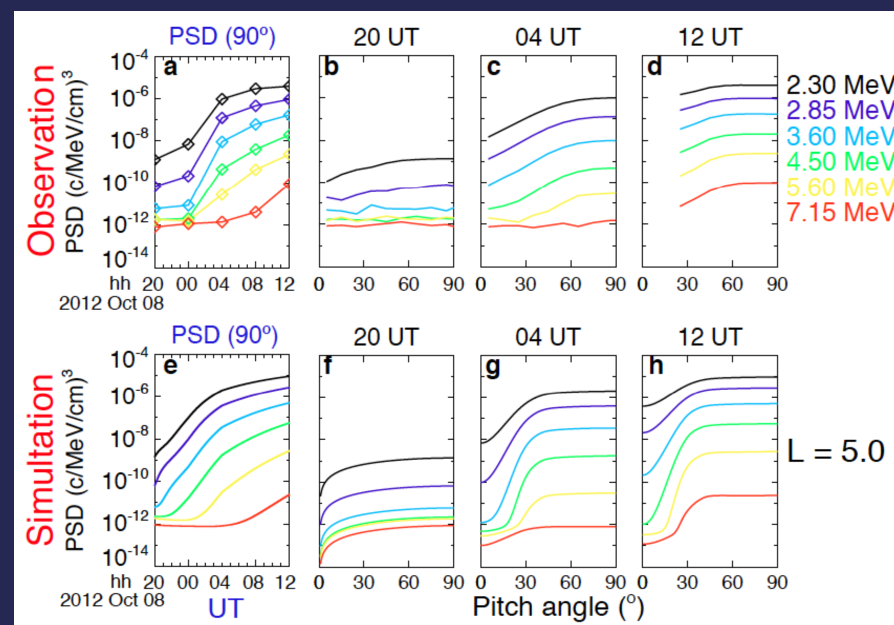

Particle Trajectories of Ring Current and Radiation Belt Particles

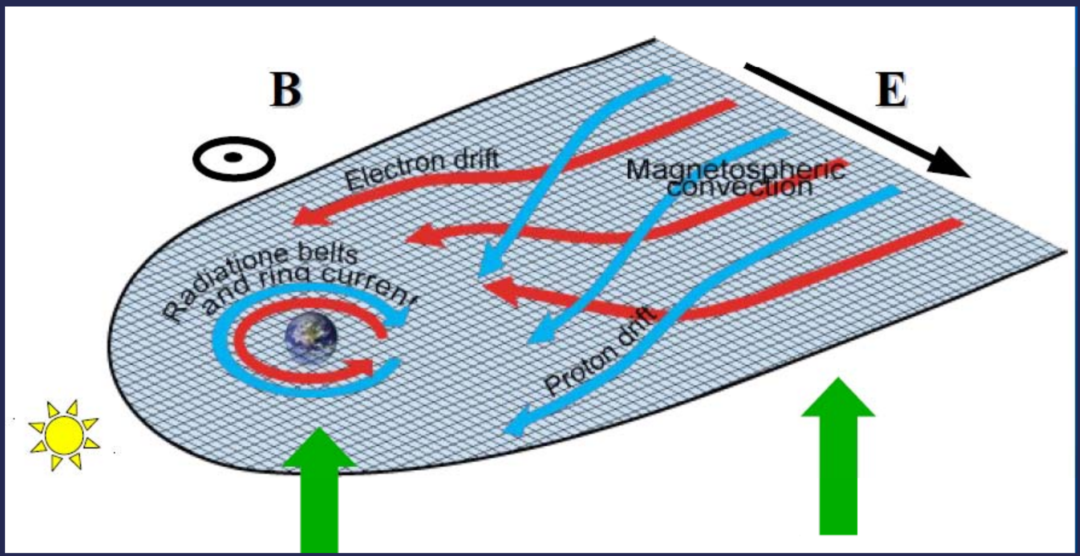

Stably trapped particles

Convection of the seed population of energetic electrons

Drift of lower energy particles is dominated by ExB drift.

Radiation Belt particles are subject to the gradient and curvature drifts and will drift around the Earth.

Electrons –eastward,

Ions-westward.

[Subbotin, et al., 2011]

Block diagram showing data exchange between the modules of the VERB 4D code.

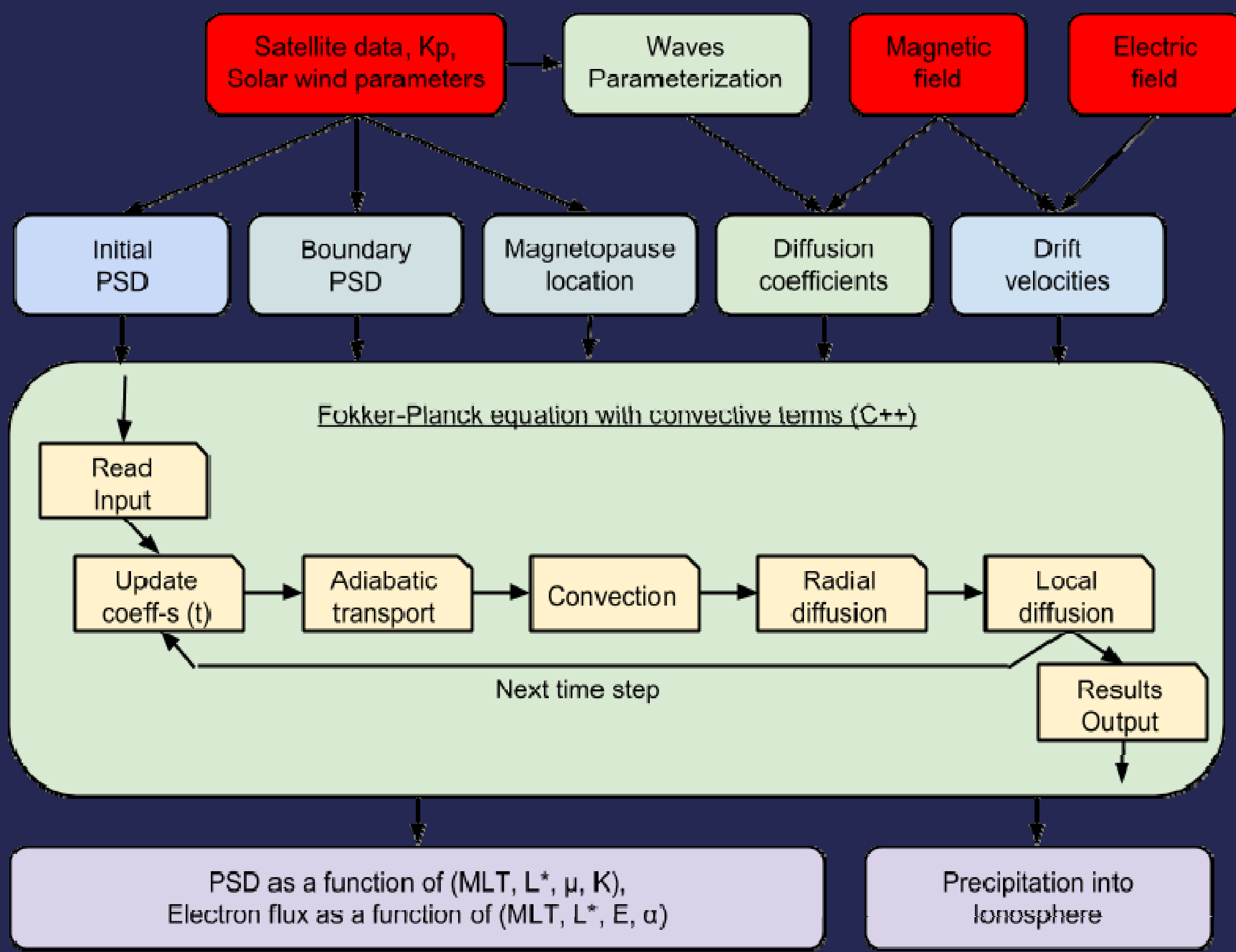

MLT-Distribution of Electrons

Starting from an empty magnitosphere, we run simulation for 1 day with Kp=6 to demonstrate the difference between convection only, convection and radial diffusion, and convection, radial, and local diffusion. PSD of μ=100 MeV/G, K=0.025 $G^{0.5}$ R_E electrons is plotted.

Convection only

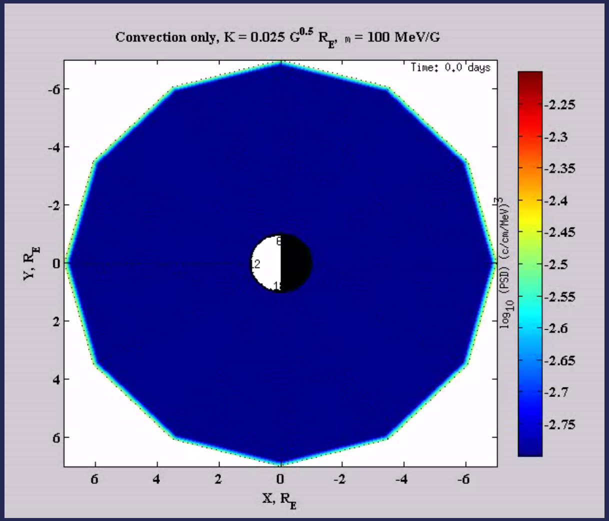

Convection and radial diffusion

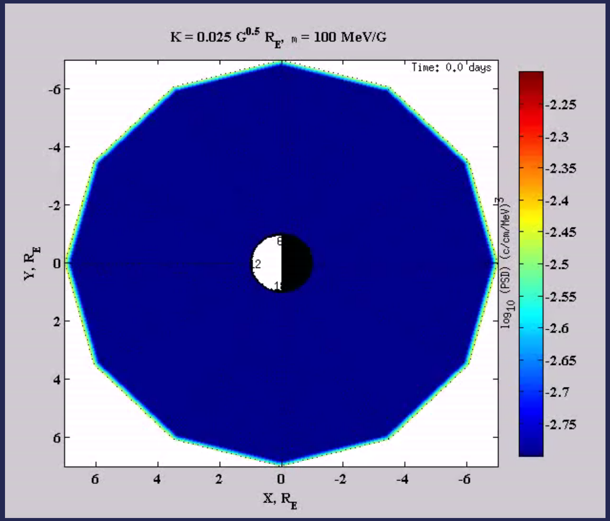

Convection, radial, and local diffusion

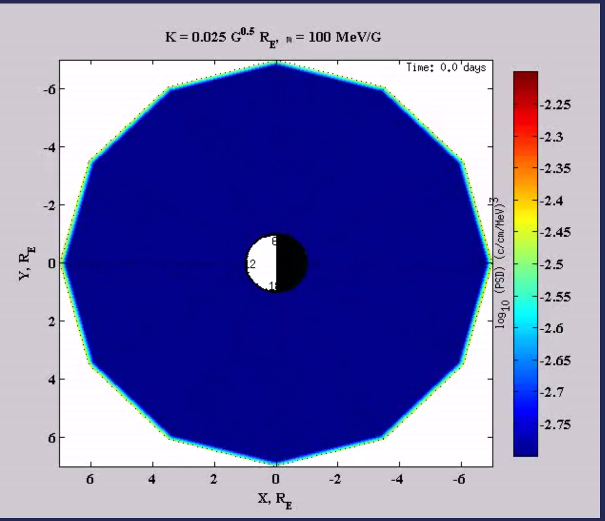

Drift Shell Splitting

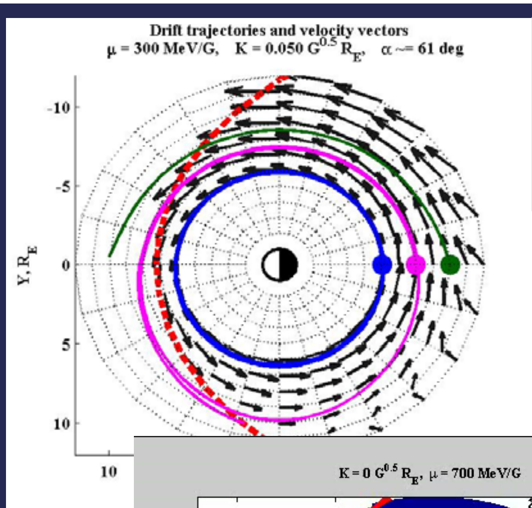

Dipole magnetic field

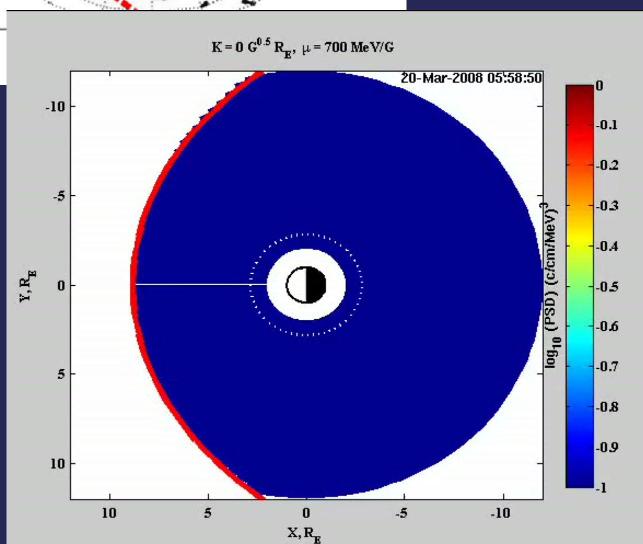

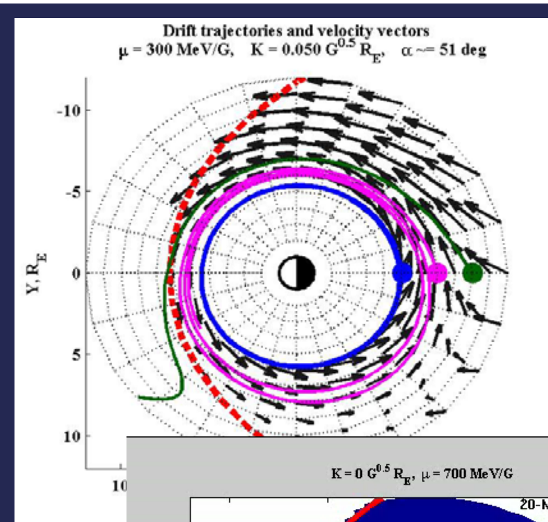

T89 magnetic field

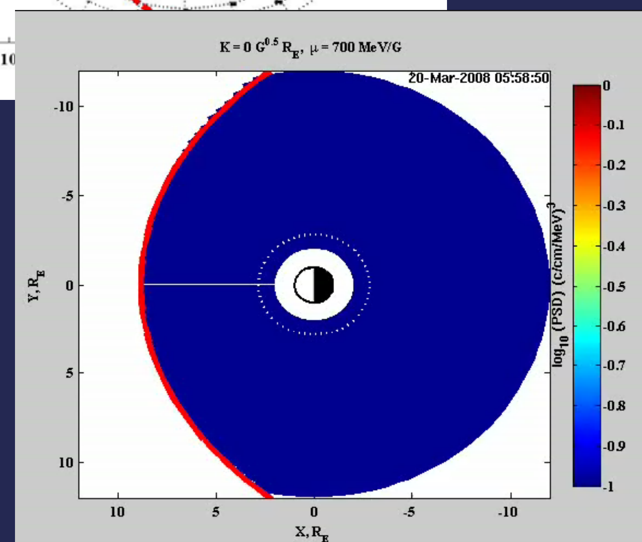

Simulations of the March 2013 Storm

Ring current 10 MeV/G

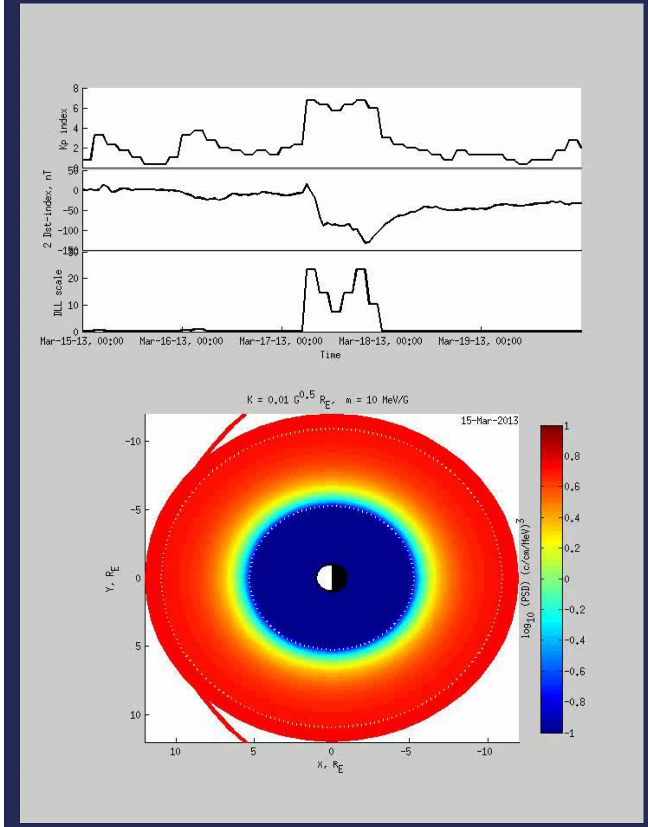

Transitional Energies
100 MeV/G

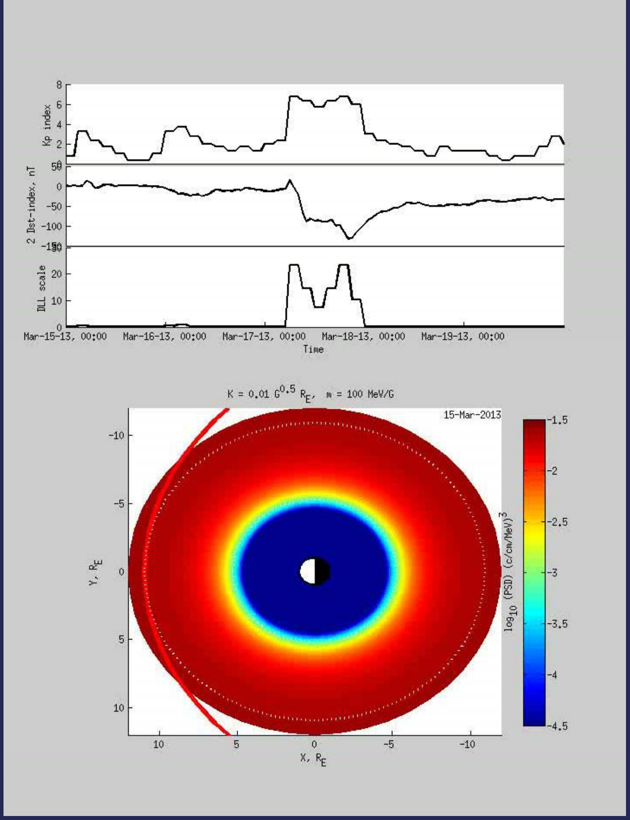

Radiation Belts 700 MeV/G

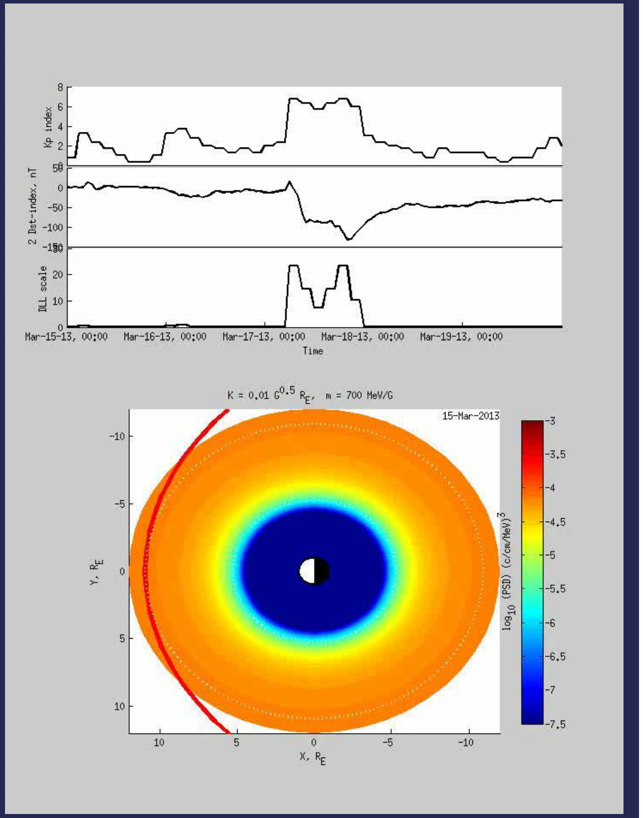

Summary

- Dynamics of the radiation belts is driven by the radial, pitch-angle, energy, and mixed diffusion due to various ULF, VLF, and ELF waves. Radial diffusion and loss determine the structure of the quiet time radiation belts. During storms local acceleration and loss to MP due to the outward radial diffusion play a crucial role.

- Different physical processes operate at ultra-relativistic energies. We can not simply consider relativistic electrons as a bulk population above 1 MeV.

- We need to better understand acceleration mechanisms that are important at ultra-relativistic energies.

Modeling Summary

- **VERB can capture the dynamics of the relativistic electrons during long term simulations as well as observations of the unusual behavior of the radiation belts during Halloween storms, and formation of the storage ring.**

- **We have now developed a 4D code that combines diffusion and convection.**

- **Future work should include combined convection and diffusion simulations in a self-consistent magnetic and electric fields provided by kinetic and global codes.**